

## Supporting Information

# Synthesis of Atomically Precise Ag<sub>16</sub> Nanoclusters and Investigating Solvent-Dependent Ultrafast Relaxation Dynamics

Sikta Chakraborty<sup>1</sup>, Sarita Kolay<sup>1</sup>, Amitava Patra<sup>1,2\*</sup>

<sup>1</sup>School of Materials Sciences, Indian Association for the Cultivation of Science,  
Kolkata 700032, India

<sup>2</sup>Institute of Nano Science and Technology, Knowledge City, Sector 81, Mohali 140306,  
India

\*Author to whom correspondence should be addressed. Electronic mail: [msap@iacs.res.in](mailto:msap@iacs.res.in)  
Telephone: (91)-33-2473-4971. Fax: (91)-33-2473-2805

<b>Contents</b>	<b>Page No.</b>
<b>Experimental Section</b>	S3-S5
<b>Fig. S1.</b> TEM image of Ag-PDT NCs	S6
<b>Fig. S2.</b> FTIR spectra of PDT ligand and Ag-PDT NCs	S6
<b>Fig. S3.</b> <sup>1</sup> H NMR of PDT ligand	S7
<b>Fig. S4.</b> <sup>1</sup> H NMR of Ag-PDT NCs	S7
<b>Fig. S5.</b> <sup>31</sup> P NMR spectra of PPh <sub>3</sub>	S8
<b>Fig. S6.</b> <sup>31</sup> P NMR spectra of Ag-PDT NCs	S8
<b>Fig. S7:</b> <sup>1</sup> H NMR spectra of PPh <sub>3</sub> .	S9
<b>Fig. S8.</b> UV-Vis absorption spectra for control experiments of Ag-PDT NCs	S9
<b>Fig. S9.</b> UV-Vis absorption spectra and emission spectra for PDT and PT capped Ag NCs	S10
<b>Fig. S10.</b> Excitation-dependent emission spectra and TCSPC data at different excitations of Ag-PDT NCs	S10
<b>Fig. S11.</b> XPS survey spectrum and Ag 3d spectrum of Ag-PDT NCs.	S11
<b>Fig. S12.</b> XPS spectrum of S of Ag-PDT NCs.	S11
<b>Fig. S13.</b> Population profile of Ag-PDT NCs in DCM	S12
<b>Fig. S14.</b> Evolution-associated decay spectra, Population profile, Kinetic traces at a selected wavelength, and TA spectra at different time delays of Ag-PDT NCs in DMF	S12
<b>Table S1.</b> Table summarising the time constants	S13
<b>Fig. S15.</b> Kinetic traces at 530 nm of Ag-PDT NCs in DCM and DMF	S13
<b>Fig. S16.</b> UV-Vis-NIR spectra of Ag-PDT NCs in DMF and DCM.	S14
<b>Fig. S17.</b> PL spectra of Ag-PDT NCs in DCM and DMF with the same optical density.	S14
<b>Fig. S18.</b> XPS spectra of Ag 3d in DCM and DMF solution of Ag-PDT NCs.	S15
<b>Fig. S19.</b> Absorption and emission spectra comparison for stability of Ag-PDT NCs	S15
<b>References</b>	S16

## EXPERIMENTAL SECTION

**Materials:** Silver nitrate ( $\text{AgNO}_3$ ), pentane-1,5-dithiol (PDT), and triphenyl phosphine (TPP) were purchased from Sigma Aldrich. Sodium borohydride ( $\text{NaBH}_4$ ), methanol (MeOH), and dichloromethane (DCM) were obtained from Merck. All the solvents used here are in spectroscopic grade, and throughout the process, Milli-Q ( $18.3 \text{ M}\Omega$ ) water was used.

**Synthesis of Ag-PDT NCs:** 10 mg  $\text{AgNO}_3$  was taken in a round bottom flask (RB) dissolved in 2 mL MeOH solution and sonicated for 2 minutes in ice-cold condition. After that, 5 mL of DCM was added to the solution. Then, 20  $\mu\text{L}$  PDT ligand was added to the solution. A white precipitate was instantly formed, confirming the formation of the metal-ligand complex. After 5 minutes,  $\text{PPh}_3$  was added (100 mg in 500  $\mu\text{L}$  DCM), and the solution became transparent. After 15 minutes, 150  $\mu\text{L}$  freshly prepared  $\text{NaBH}_4$  was added (10.5 mg in 500  $\mu\text{L}$  ice-cold  $\text{H}_2\text{O}$ ). The solution instantly turned pale yellow after  $\text{NaBH}_4$  addition, and with time, it turned to a deep brown color. The reaction was allowed to stir for 3 h in an ice bath ( $\sim 0^\circ \text{C}$ ).

**Purification:** After 3h, the brown color solution was washed with water. After that, the solution was centrifuged for 8 minutes at 10000 rpm. Then, the supernatant was collected through filtration. The solution then rotary evaporated and finally dissolved in DCM. For TGA analysis, the solution was precipitated out using diethyl ether solvent after rotary evaporation treatment. After centrifugation, the solution was washed with hexane and dried before the experiment.

**Instrumentation:** Room temperature optical absorption spectra were carried out with a UV-vis spectrophotometer (Shimadzu) using a cuvette with a path length of 1 cm. The UV-Vis-NIR spectra were performed on a Cary 5000 (Agilent) instrument. The detectors used here were PMT and PbSmart NIR detectors. The PL spectra of all the samples were taken with a fluoroMax-P (HORIBA Jobin Yvon). The mass of the Ag-NCs was analyzed by Maldi-TOF mass spectrometry on a Bruker Deltonics Autoflex II TOF/TOF system using a 337 nm pulse laser source. The saturated solution of the DCTB (trans-2-[3-(4-tert-butylphenyl)-2-methyl-2-propenylidene]malononitrile) matrix was used with NCs in a 100:1 ratio to determine the mass. The sample was dissolved in MeOH and high-resolution mass spectrometry was performed in a Waters micromass Q-TOF micro-MS system by an electrospray ionization (ESI-MS) technique. TA-SDQ Q-600 thermal analyser was used to collect the data for TGA. The X-ray photoelectron spectroscopy (XPS) was obtained using the Omicron Nanotechnology

instrument to determine the binding energy. The  $^1\text{H}$  NMR spectra were recorded on Bruker AVANCE III 400 MHz in  $\text{CDCl}_3$  ( $\delta$  7.26 ppm).  $^{31}\text{P}$  NMR spectra were obtained from Bruker AVANCE REO-600 MHz instrument. In this case,  $\text{CDCl}_3$  ( $\delta$  7.26 ppm) was used also. Fourier-transform infrared (FTIR) spectroscopy was performed on a Shimadzu-made FTIR-8300 spectrometer using KBr pellets. The transmission electron microscopy (TEM) experiment used a JEOL-JEM-2100M transmission electron microscopy system. The TEM samples were prepared by drop-casting the cluster solutions onto the copper grid covered by a carbon film. For time-correlated single-photon counting (TCSPC) measurement, the samples were excited at 405 nm using a Nano LED light source on DeltaFlex Modular Fluorescence Lifetime System. A picosecond photon detection (PPD) module collected all the fluorescence decays with spectral response 230nm-850 nm. Equation 1 was used to analyze the experimental time-resolved fluorescence decays,  $P(t)$ :

$$P(t) = b + \sum_i^n \alpha_i \left( -\frac{t}{\tau_i} \right) \quad (1)$$

Here,  $n$  represents the number of emissive species,  $b$  is for baseline correction,  $\alpha_i$  is the pre-exponential factor, and  $\tau_i$  is the excited-state fluorescence decay time associated with the  $i^{\text{th}}$  component. The average decay time  $\langle \tau \rangle$  was calculated using the following equation

$$\langle \tau \rangle = \sum_{i=1}^n \beta_i \tau_i \quad (2)$$

Where  $\beta_i = \alpha_i / \sum \alpha_i$  and  $\beta_i$  are the contribution of the decay component.<sup>1</sup> The quantum yield (QY) of the NCs was measured using Rhodamine B in 0.2 % ethanol solution as reference dye using the following equation

$$QY_s = (F_s \times A_r \times \eta_s^2 \times QY_r) / (F_r \times A_s \times \eta_r^2) \quad (3)$$

$F_s$  and  $F_r$  are the integrated fluorescence emission of the sample and the reference, respectively.  $A_s$  and  $A_r$  are the absorbance of the sample and the reference, respectively, at the excitation wavelength.  $QY_s$  and  $QY_r$  are the quantum yield of the sample and reference ( $QY_r=0.97$ ).<sup>1</sup> The refractive index ( $\eta$ ) of DCM, DMF, and ethanol are 1.42, 1.43, and 1.36, respectively. The absorbance values are kept smaller than 0.05 at the excitation wavelength to minimize the self-absorption effect of the samples.

### Transient Absorption Spectroscopy

Transient absorption data were collected using a femtosecond transient absorption spectrophotometer (TAS). This instrument setup consists of a mode-locked Ti: sapphire oscillator (Seed laser, Spectra-Physics Mai-tai SP) to generate pulses of  $\sim 80$  fs duration with a wavelength of 800 nm at a repetition rate of 80 MHz. A separate pump laser (Nd: YLF Laser, 527 nm, Spectra-Physics Empower 45) supplies the energy required for amplifying the seed pulse. The Spitfire ace amplifier system (consisting of the optical stretcher, regenerative amplifier, and optical compressor) amplifies low-energy ( $\mu\text{J}$ ) laser pulses to high energy (mJ). The output from the amplifier (800 nm,  $\sim 100$  fs, 1 kHz, 2.5 mJ pulse energy) is directly delivered to the spectrophotometer. This output was split into two portions using a beam splitter: one for pump pulse and the other one for probe pulse generation. One part is driven to a BBO crystal, which generates a 400 nm pump beam by second harmonic generation for exciting the samples. The other part of the 800 nm light is pointed on a  $\text{CaF}_2$  plate to produce a white-light continuum (WLC) used as a probe pulse. The white-light continuum is divided into two parts; one acts as a probe pulse, and the other acts as a reference. The reference and transmitted probe beams are passed to different diode arrays, where the reference beam assists in accounting for the intensity fluctuation in the white-light continuum. To avoid sample degradation and multiexciton effect, the power of the pump pulse is kept low enough ( $< 5 \mu\text{J}/\text{cm}^2$ ). All recorded data are fitted using Surface Explorer version 4.0 software for single wavelength fitting and GloTarAn version 1.5.1 software for Global analysis.<sup>2-4</sup> Subsequently, the chirp is corrected to remove the group velocity dispersion (GVD). Any time component less than 100 fs is pulse width limited and can be treated as an instrument response function. We have globally analyzed the data by using a kinetic model which consists of sequentially interconverting Evolution Associated Difference Spectra (EADS), e.g.,  $1 \rightarrow 2 \rightarrow 3 \rightarrow 4 \rightarrow 5 \rightarrow \dots$ . The arrows indicate successive mono-exponential decays of increasing time constants. These time constants can be considered as the lifetime of each EADS. Extra correlated structures in the residuals are eliminated by choosing the minimum required numbers of kinetic components with the help of SVD analysis. This procedure depicts the evolution of the (excited) states of the system.

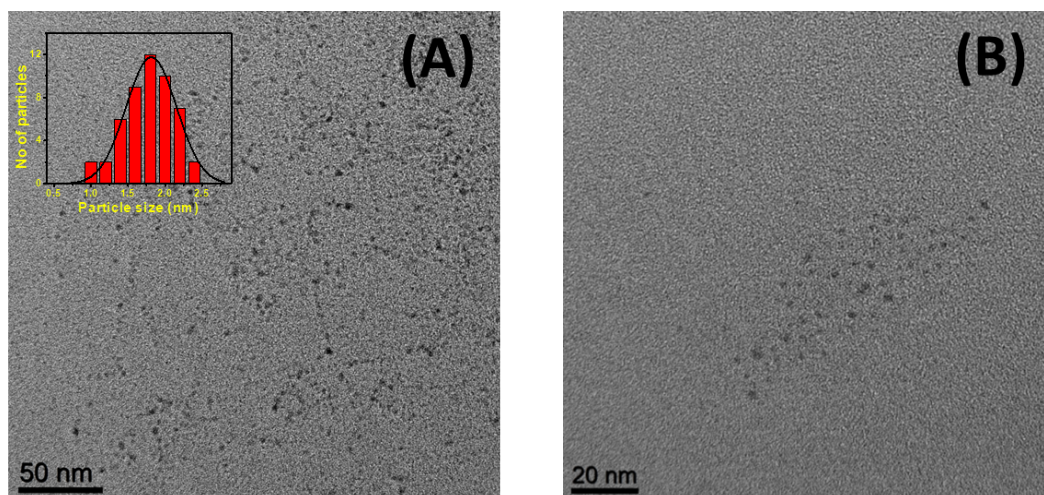


**Fig. S1:** TEM images of Ag-PDT NCs in (A) 50 nm (inset represents the size distribution) and (B) 20 nm scales.

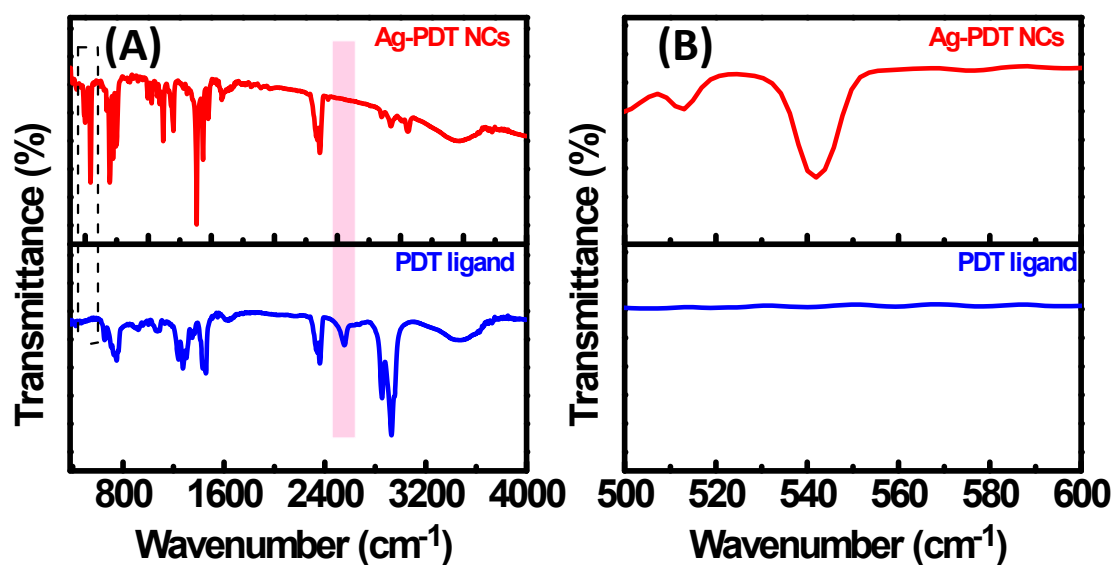


**Fig. S2:** FTIR spectra of PDT ligand and Ag-PDT NCs (A) from 400 - 4000  $\text{cm}^{-1}$  and (B) from 500-600  $\text{cm}^{-1}$ .

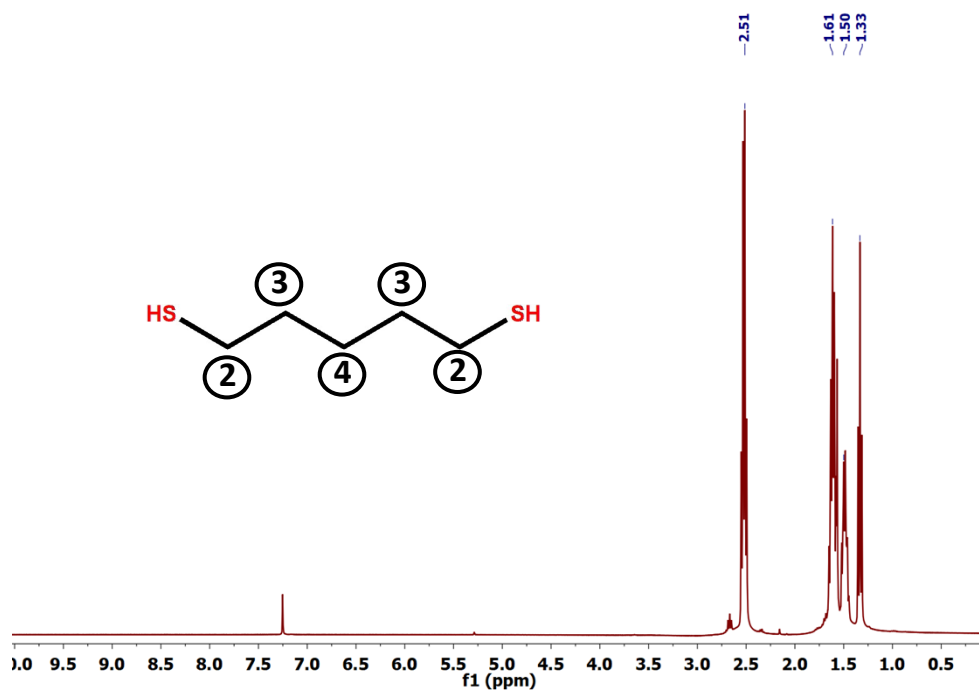


**Fig. S3:** <sup>1</sup>H NMR spectrum of PDT ligand

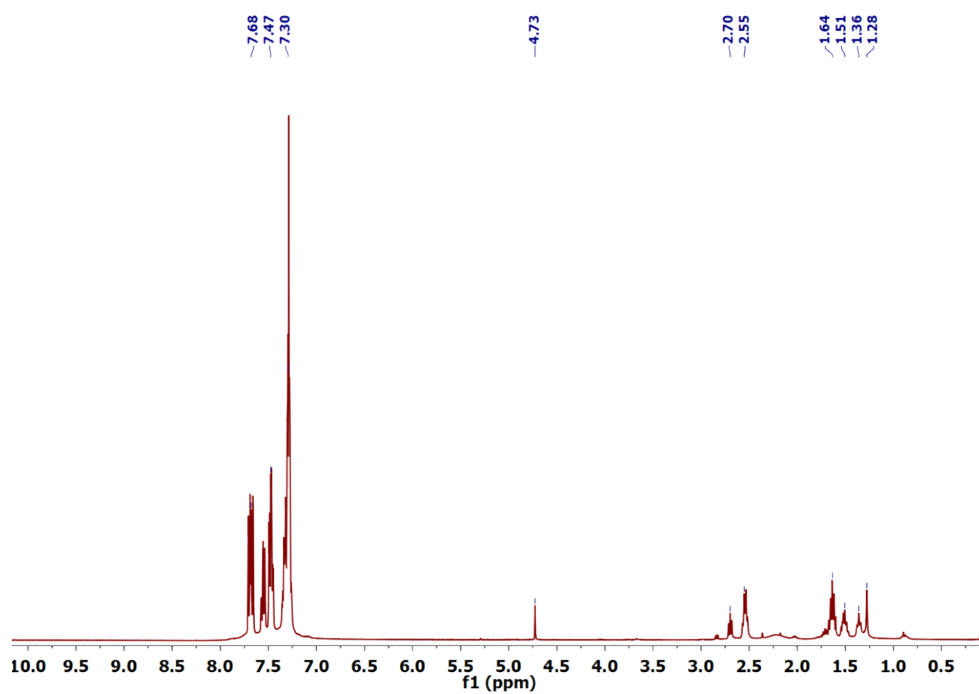


**Fig. S4:** <sup>1</sup>H NMR spectrum of Ag-PDT NCs

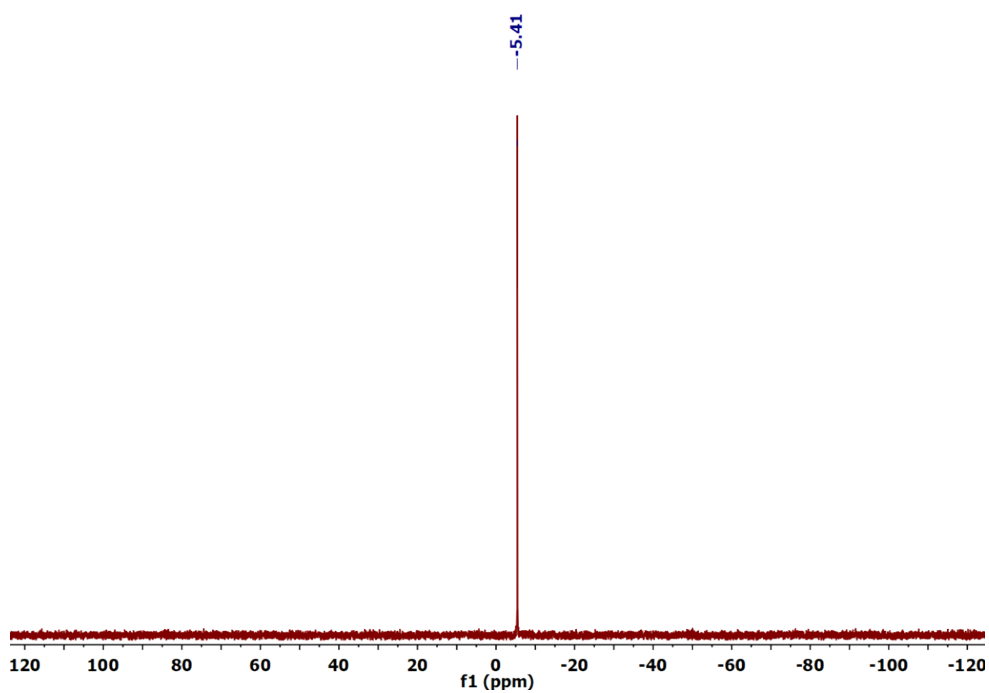


**Fig. S5:**  $^{31}\text{P}$  NMR spectrum of  $\text{PPh}_3$ .

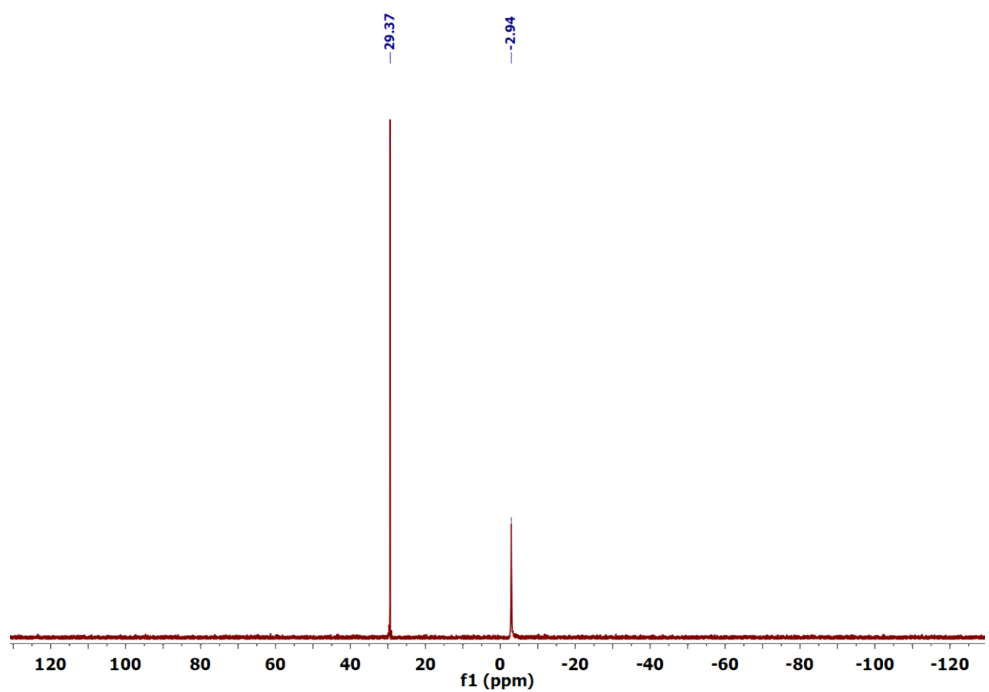


**Fig. S6:**  $^{31}\text{P}$  NMR spectrum of Ag-PDT NCs.



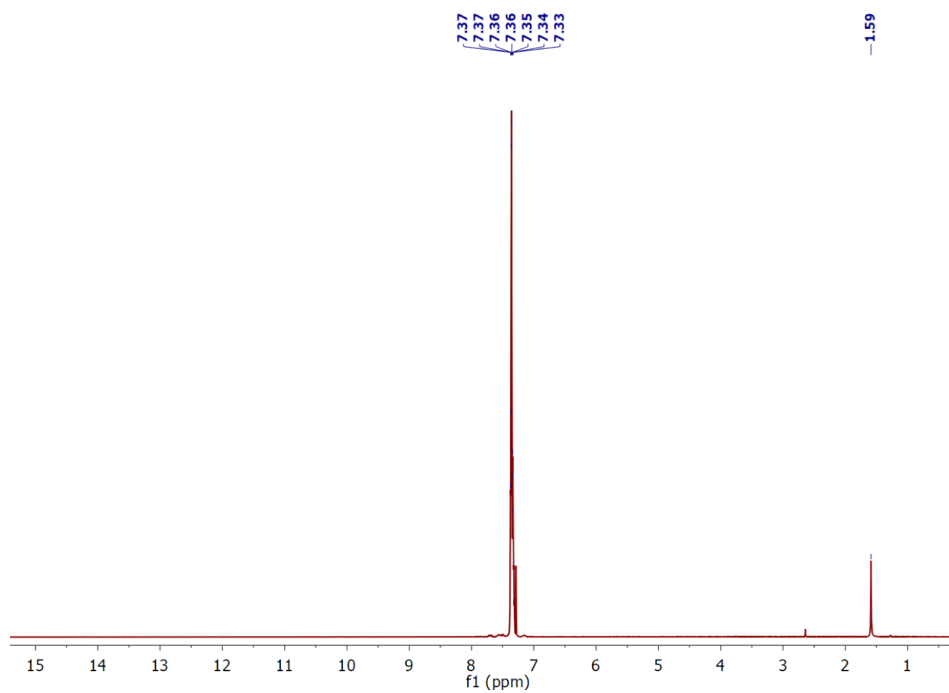


**Fig. S7:**  $^1\text{H}$  NMR spectrum of  $\text{PPh}_3$ .

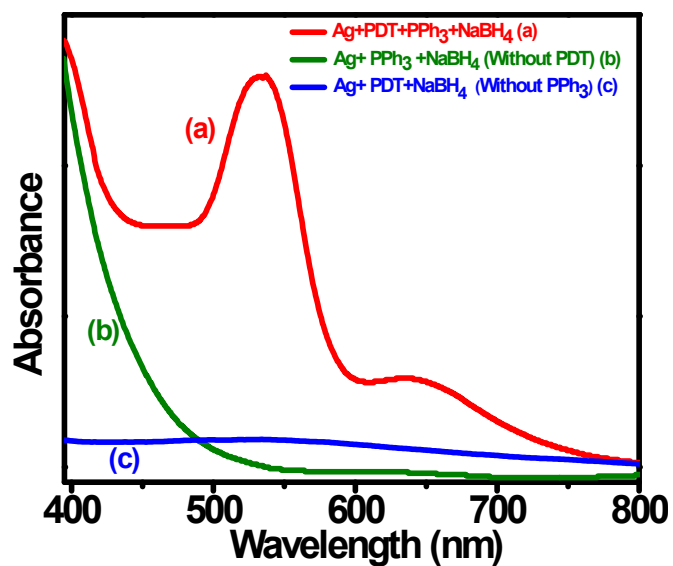


**Fig. S8:** UV-Vis absorption spectra for control experiment of (a)  $\text{Ag}^+$  PDT +  $\text{PPh}_3$ + $\text{NaBH}_4$ , (b)  $\text{Ag}^+$   $\text{PPh}_3$ +  $\text{NaBH}_4$ , and (c)  $\text{Ag}^+$  PDT+  $\text{NaBH}_4$ .

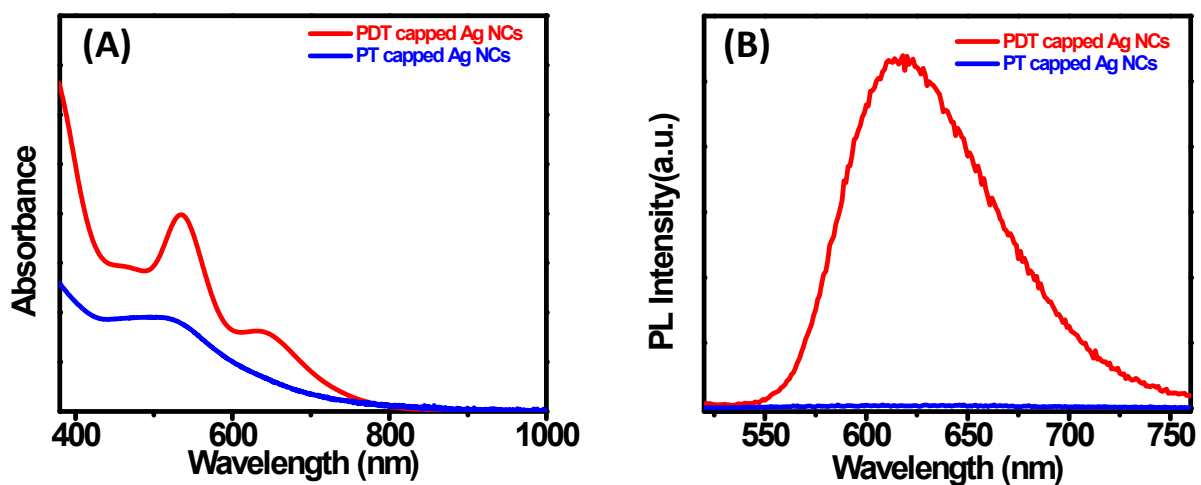


Fig. S9: (A) UV-Vis absorption spectra and (B) Emission spectra for PDT and PT capped Ag NCs

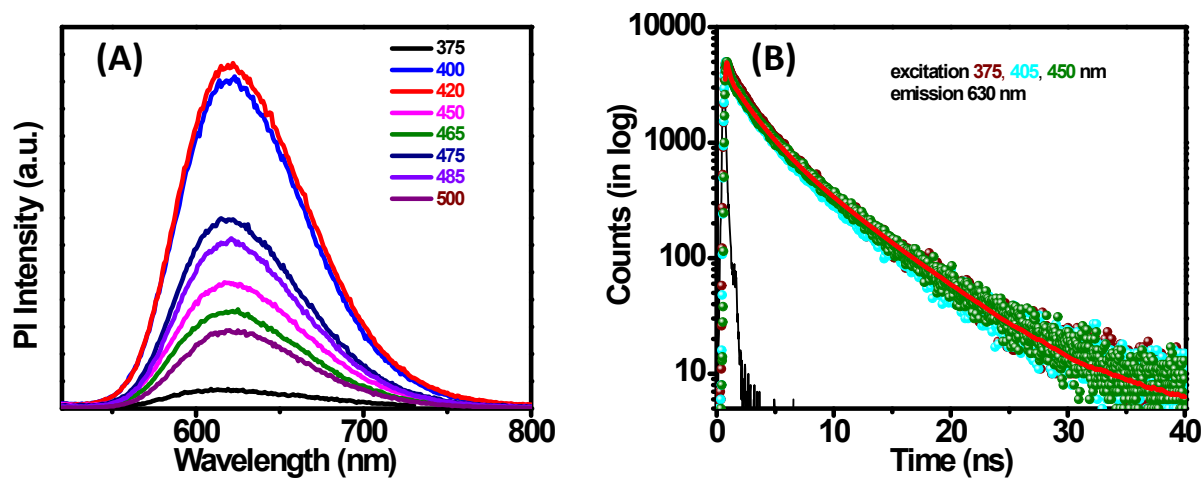


Fig. S10: (A) Excitation-dependent emission spectra and (B) TCSPC data at different excitations of Ag-PDT NCs

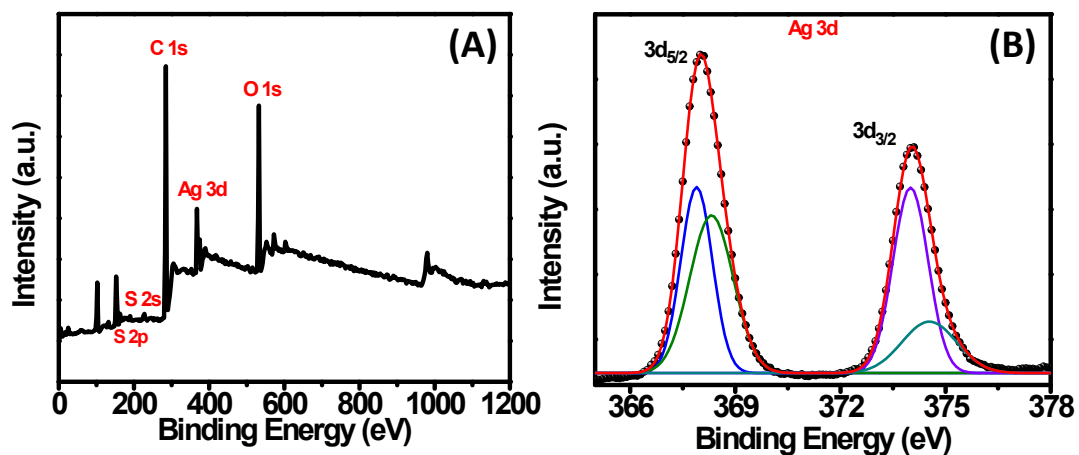


Fig. S11: (A) XPS spectrum and (B) Ag 3d spectrum of Ag-PDT NCs

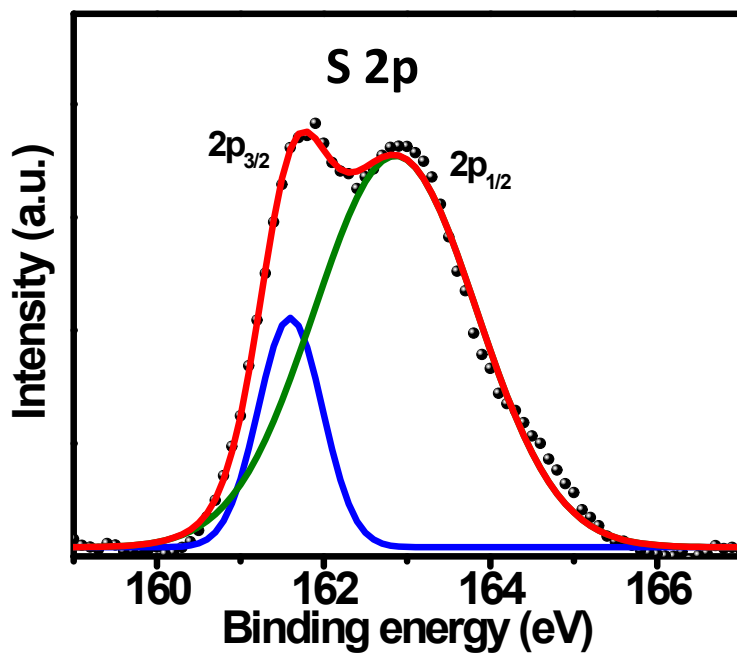


Fig. S12: XPS spectrum of S 2p of Ag-PDT NCs.

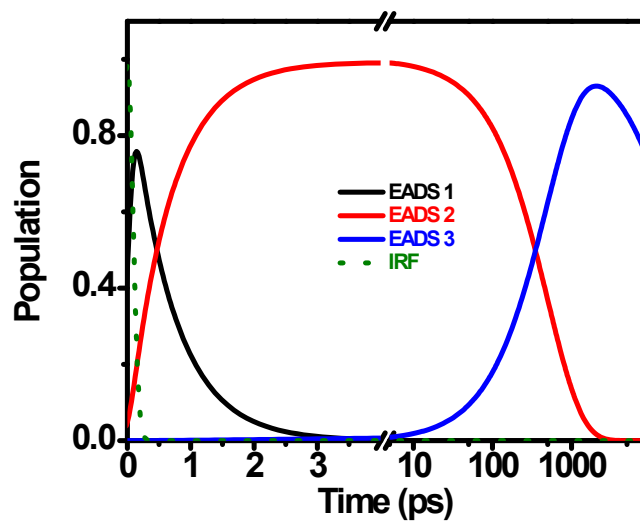


Fig. S13: Population profiles of Ag-PDT NCs in DCM

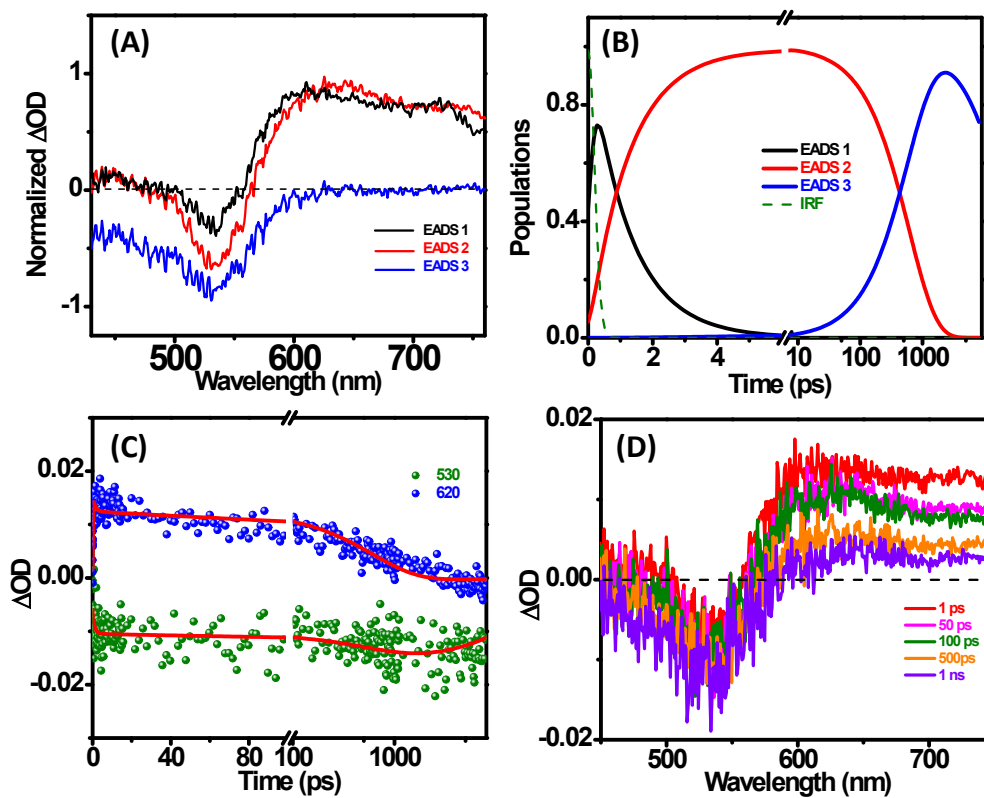
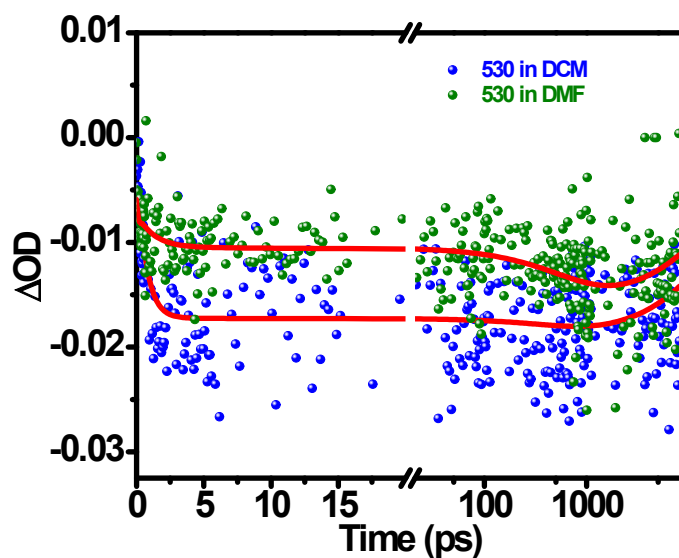


Fig. S14: (A) Evolution-associated decay spectra, (B) Population profiles of Ag-PDT NCs, (C) Kinetic traces at a selected wavelength, and (D) TA spectra at different time delays of Ag-PDT NCs in DMF.

**Table S1:** The time components obtained from the global fitting for Ag-PDT NCs in both DCM and DMF are illustrated below-

Systems	$\tau_1$	$\tau_2$	$\tau_3$
Ag-PDT NCs in DCM	664 fs	500 ps	> 1 ns
Ag-PDT NCs in DMF	1.25 ps	624.25 ps	> 1 ns



**Fig. S15:** Kinetic traces at 530 nm of Ag-PDT NCs in DCM and DMF.

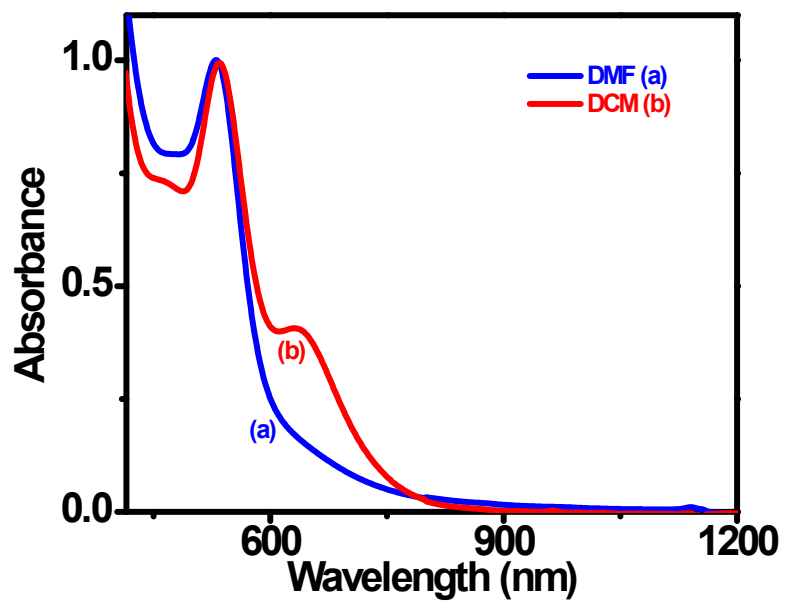


**Fig. S16:** UV-Vis-NIR spectra of Ag-PDT NCs in (a) DMF and (b) DCM.

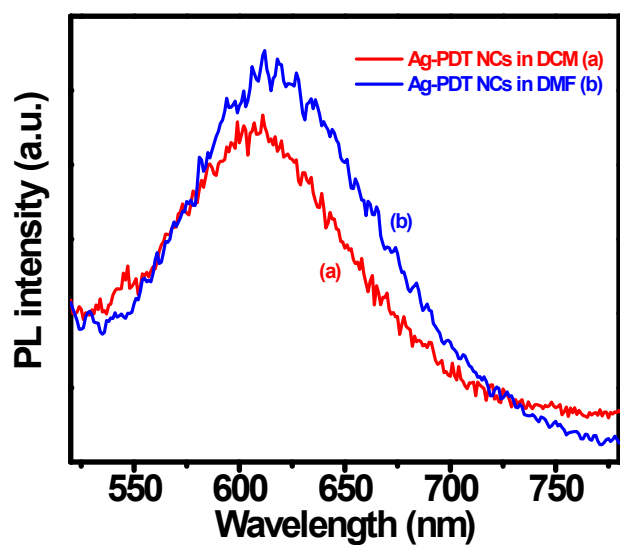


**Fig. S17:** PL spectra of Ag-PDT NCs in (a) DCM and (b) DMF with the same optical density.

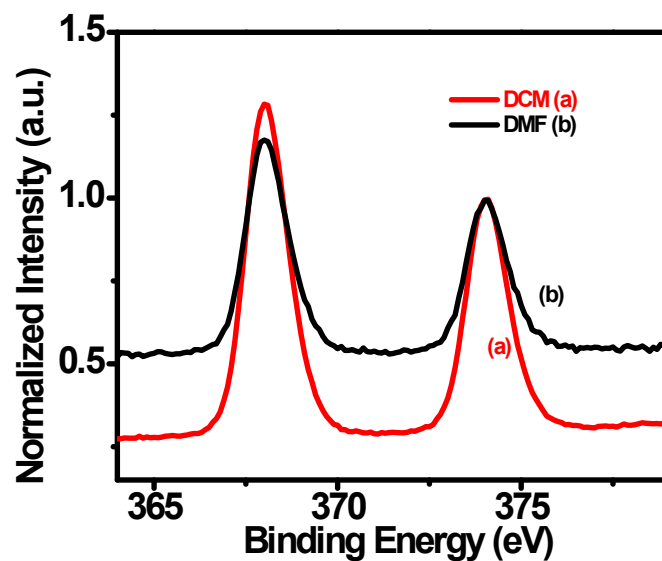


**Fig. S18:** XPS spectra of Ag 3d in (a) DCM and (b) DMF solution of Ag-PDT NCs.

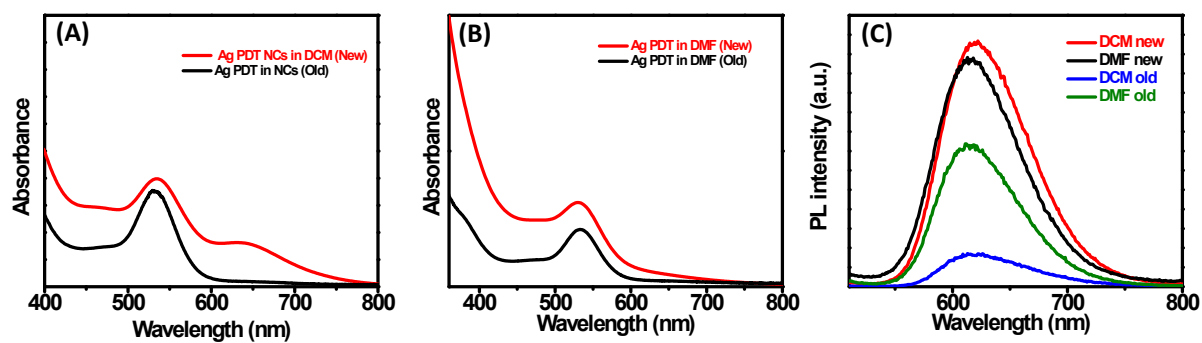


**Fig. S19:** Absorption spectra of Ag PDT in (A) DCM and (B) DMF and (C) Emission spectra of Ag PDT NCs in DCM and DMF

## References

1. J. R. Lakowicz, 3rd ed.; Springer, **2006**.
2. I. H. M. van Stokkum, D. S. Larsen and R. van Grondelle, *Biochim. Biophys. Acta*, 2004, **1657**, 82-104.
3. J. J. Snellenburg, S. Laptenok, R. Seger, K. M. Mullen and I. H. M. van Stokkum, *J. Stat. Softw.*, 2012, **49**, 1 - 22.
4. K. M. Mullen and I. H. M. van Stokkum, *J. Stat. Softw.*, 2007, **18**, 1 - 5.